A R C H I V E S O F M E T A L L U R G Y A N D M A T E R I A L S
Volume 60 2015 Issue 3
DOI: 10.1515/amm-2015-0344

A. M. EL-NAGGAR*,**, A. A. ALBASSAM*, K. OŹGA***,#, M. SZOTA****, I.V. KITYK***

UV-INDUCED ANISOTROPY IN $CdBr_2$-$CdBr_2$: Cu NANOSTRUCTURES

ANIZOTROPIA WYWOŁANA PROMIENIOWANIEM UV W NANOSTRUKTURACH $CdBr_2$-$CdBr_2$: Cu

We have found an occurrence of anisotropy in the nanostructure $CdBr_2$-$CdBr_2$: Cu nanocrystalline films. The film thickness was varied from 4 nm up to 80 nm. The films were prepared by successive deposition of the novel layers onto the basic nanocrystals. The detection of anisotropy was performed by occurrence of anisotropy in the polarized light at 633 nm He-Ne laser wavelength. The occurrence of anisotropy was substantially dependent on the film thickness and the photoinduced power density. Possible mechanisms of the observed phenomena are discussed.
Keywords: $CdBr_2$-$CdBr_2$: Cu nanocrystalline film, UV-induced anisotropy, optical properties, birefringence, layered crystals.

Wykryto pojawienie się anizotropii w nanostrukturalnych warstwach nanokrystalicznych $CdBr_2$-$CdBr_2$: Cu. Grubość warstwy zmieniano w zakresie od 4 nm do 80 nm. Nanostrukturalne warstwy otrzymano poprzez kolejne osadzanie na nowych warstwach na podstawie nanokrystalitów. Detekcję anizotropii wykonano w spolaryzowanym świetle lasera gazowego He-Ne o długości fali 633 nm. Anizotropia optyczna występująca w warstwach w znacznym stopniu zależy od grubości warstwy i gęstości mocy indukowanej światłem. Omówiono możliwe mechanizmy obserwowanego zjawiska.

1. Introduction

The optically operated devices like optical triggers [1-4] requires intensive search of materials possessing high sensitivity to laser light. Particular interest presents the UV-operated devices [5]. The materials used require fast changes after illumination by the sufficiently lower power laser densities. After the such formed changes the occurred anisotropy should relatively quickly relax. The different materials were used for this goal [6], however all the materials requires a finding of materials which may create a maxima anisotropy at the lowest possible power densities [7-9]. One of a way of enhancement of such efficiency is a formation of the nanostructured composites [10, 11]. Very technological here seem to be the layered crystals of Cd halogenides [12]. The mentioned crystals are able to be cleaved up to the thickness about several nm and it is occurs a possibility to cover layer by layer by relatively simple growth from aqueous solution [13]. The control of the thickness may be performed directly during the growth.

Additionally during the growth we will deposit the after of the $CdBr_2$: Cu with the same thickness as the initial level. We will register the changes of the anisotropy in the sequence perpendicularly to the probing beam and we will additionally study the relaxation after the switching off of the photoinduced laser beam. Due to relatively large energy gap of the $CdBr_2$ crystals (about 4 eV) we were able to sue the nitrogen laser with wavelength 337 nm. The doping was about 0.5 % which does not change the absorption substantially.

2. Experimental

The titled nano-heterostructures were synthesized by a slow evaporation of aqueous solution of the $CdBr_2$ solutes in the water. The thickness was controlled during the growth process by changes of the optical path on the border crystallites and without the crystal. After that the crystallites were put in the aqueous solution in the $CdBr_2$: Cu (1 %). The crystals were take off of the solution and their thickness was dependent on the time of evaporation. For the studies we have picked up the crystals with sizes 4 nm, 7 nm, 12 nm, 19 nm, 50 nm and 80

* RESEARCH CHAIR OF EXPLOITATION OF RENEWABLE ENERGY APPLICATIONS IN SAUDI ARABIA, PHYSICS & ASTRONOMY DEPT., COLLEGE OF SCIENCE, KING SAUD UNIVERSITY, P.0.BOX 2455, RIYADH 11451, SAUDI ARABIA
** PHYSICS DEPARTMENT, FACULTY OF SCIENCE, AIN SHAMS UNIVERSITY, ABASSIA, CAIRO 11566, EGYPT.
*** CZESTOCHOWA UNIVERSITY OF TECHNOLOGY, INSTITUTE OF ELECTRONIC AND CONTROL SYSTEM, 17 ARMII KRAJOWEJ AV., 42-200 CZESTOCHOWA, POLAND
**** CZESTOCHOWA UNIVERSITY OF TECHNOLOGY, INSTITUTE OF MATERIAL SCIENCE ENGINEERING, 19 ARMII KRAJOWEJ AV., 42-200 CZESTOCHOWA, POLAND
# Corresponding author: cate.ozga@wp.pl

Unauthenticated
Download Date | 2/20/18 7:03 PM

nm. We have defined the energy gap following an absorption edge as described in the ref. 14. The accuracy of the energy gap definition was equal to about 0.25 eV. The results were treated within a framework of Urbach rule and have shown coexistence of direct and indirect transitions. We have established that the increasing sizes lead to decrease of the energy gap and at some relatively high sizes (more than 100 nm) it does not change. The corresponding parameters are presented in the Table 1.

TABLE 1

Energy gap parameters of the studies $CdBr_2$:$CdBr_2$: Cu nanocrystalline films versus the thickness.

Thickness [nm]	Energy gap [eV]
4	4.56
7	4.43
12	4.39
19	4.41
50	4.42
80	4.42

The sizes of the surfaces for the titled cleaved crystals were to be equal about 3-4 mm and they were put between the quartz plater in order to obtain perfect planes.

The general schema for the measurements of the photoinduced anisotropy using as a probing cw He-Ne laser with power about 20 mW is depicted in the Fig. 1.

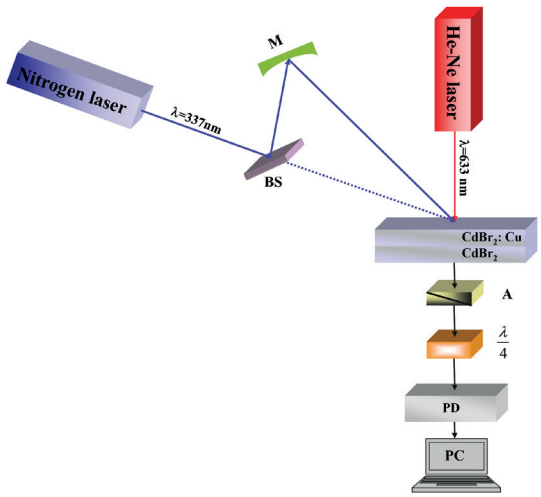

Fig. 1. Principal schema for the photoinduced changes of the birefringence in the titled nanocrystalline films: Nitrogen laser – photoinduced laser, He-Ne laser – probing laser, BS – beam splitter, M – mirror, A – analyzer, l/4 - phase plate, DP – photodetector, PC - computer persolnaly

As a photoinduced laser was used 7 ns 337 nm nitrogen laser with frequency repetition about 1500 Hz and power densities varying up to 3 GW/cm^2 which have created an anisotropy by two coherent beams incident at different angles within the 24…37 degrees. The photoinduced laser has worked in the TEM_{01} mode and its profile beam was Gaussialn-like. The two coherent beams are chosen to form some phase shift which favors an occurrence of anisotropy similarly to the grating. The two-layered nanocomposites were illuminated by the two coherent UV-induced beam and the detection allows to monitor the occurrence of anisotropy. The rotation of the analyzer allows to obtain the maximal contrast of the camera CCD. The birefringence was determined following an expression:

$$\Delta n = \frac{\lambda \phi}{d} \qquad (1)$$

where: Δn is birefringence; λ – is He-Ne laser wavelength equal to 633 nm; ϕ – phase shift angle and d – sample's thickness.

3. Results and discussion

The photoinduced anisotropy pictures for the samples with thickness 4 nm (a), 7 nm (b), 12 nm (c), 19 nm (d), 50 nm (e) and 80 nm (f), at the increase of the laser beam power up to 100 MW/cm^2 are shown in the Fig. 2 a-f. The obtained results unambiguously show that maximal anisotropy corresponding to the formation of the anisotropy is observed for the 7 nm samples (see Fig. 2b). The maximally achieved UV-induced birefringence was equal to about 3.1 $\times 10^{-4}$. The less thickness do not sufficient to form the anisotropy and the pictures are substantial asymmetric. This may be cause by some photothermal effects and the substantial non-homogenous excited carrier's re-distribution.

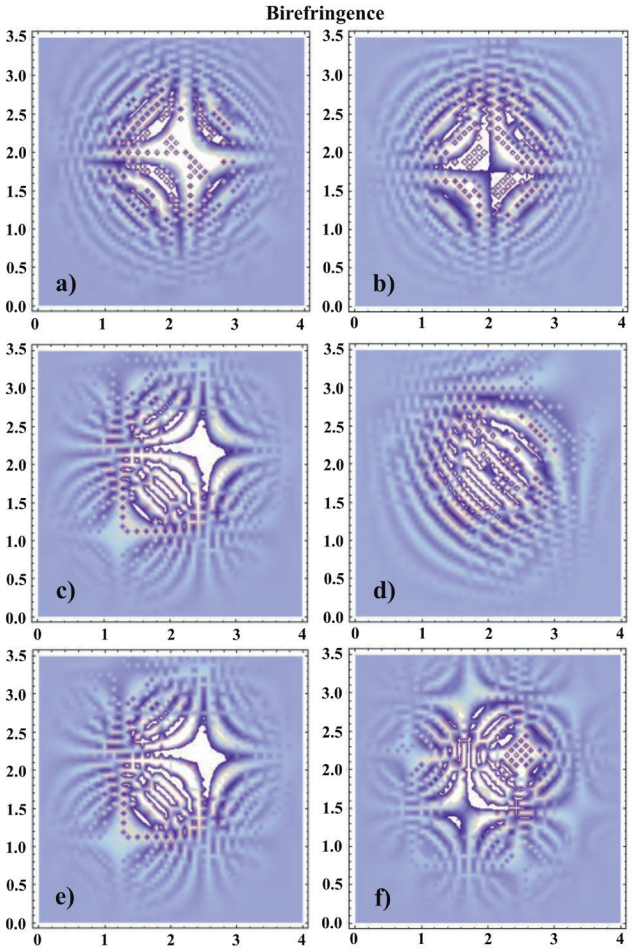

Fig. 2. The photoinduced anisotropy pictures for the samples with thickness 4 nm (a), 7 nm (b), 12 nm (c), 19 nm (d), 50 nm (e) and 80 nm (f), at the increase of the laser beam power up to 100 MW/cm^2

Unauthenticated
Download Date | 2/20/18 7:03 PM

For the samples with higher sizes the effects begin more asymmetrical with respect to anisotropy due to occurrence of the multi-time reflection and formation of several interferometric patterns. The principal is a fact that optimal UV laser power density was equal to about 100 MW/cm^2, which is sufficient to form the necessary UV-operated anisotropic optical devices. Such devices may found an application during the laser Q-switching and passive modulators. In Fig. 3 is given the time decay of the photoinduced birefringence for the nanostructure $CdBr_2$-$CdBr_2$: Cu nanocrystalline film with thickness 7 nm confirming the complete relaxation of the photoinduced changes after about 10 ms of switching off the laser treatment. This behavior was almost the same for other samples and it may reflect a principally surface dominant contribution to the observed decay.

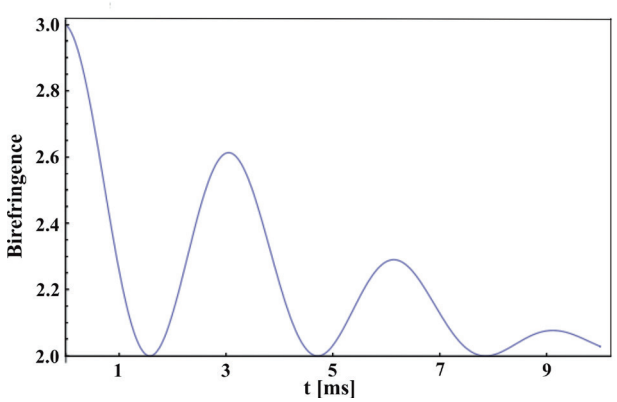

Fig. 3. Time kinetics of birefringence decay at film thickness 7 nm after 100 MW/cm^2 UV-laser treatment. Birefringence should be multiplied by 10^{-4}

For convenience of readers in the Fig. 4 is presented the maximally achieved birefringence versus the sample's different sizes. From this graph we can observed, that the achieved maximal value of the photoinduced birefringence did not exceed 3.1×10^{-4} for the nanostructure film with thickness 7 nm. The further increase of the sample thickness up to 80 nm leads to the about 40 % decrease values of the birefringence. This may be a consequence of the bulk long-range ordered photocarrier diffusion.

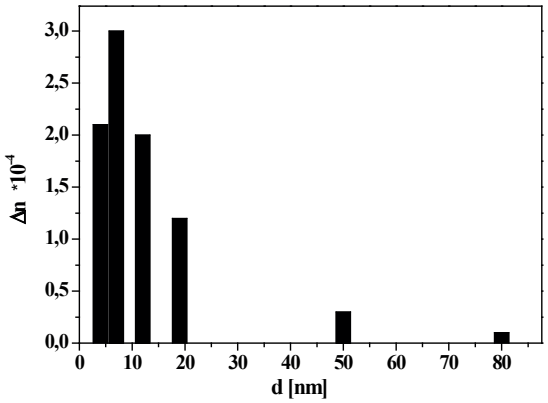

Fig. 4. Dependence of the maximally achieved birefringence versus the sample thickness

4. Conclusions

For the first time we have found photoinduced anisotropy in the nanolayers of $BdBr_2$:$CdBr_2$: Cu nanostructure. The anisotropy controlled by birefringence has shown a maximal value at nanolayer's thickness 7 nm. After switching off of the nitrogen laser photoinduced power the anisotropy shows some attenuation and quasi-periodic processes. This fact reflects a competition between the pumped free carrier and the photo-thermal waves. During the enhancement of the thickness up to 80 nm the effect disappears. So the principal role of the interfaces $CdBr_2$ and $CdBr_2$: Cu is shown.

Acknowledgements

The project was financially supported by King Saudi University, Vice Deanship of research chairs, research chair of Exploitation of Renewable Energy Applications in Saudi Arabia.

REFERENCES

[1] D. Sun, Y. Tian, Y. Zhang, Z. Xu, M.Y. Sfeir, M. Cotlet, O. Gang, Light harvesting nanoparticle core-shell clusters with controllable optical output, ACS Nano, (2015) DOI: 10.1021/nn507331z. (in press).

[2] Z. Sun, S. Li, S. Zhang, F. Dong, M. Hong, J. Lou, Nonlinear second-order optical switch of a new hydrogen-bonded supramolecular crystal with a high laser-induced damage threshold, Adv. Opt. Mater. **2** (3), 1199-1205 (2014).

[3] A-K.U. Michel, P. Zalden, D.N. Chigrin, M. Wuttig, A. M. Lindenberg, T. Taubner, Reversible optical switching of infrared antenna resonances with ultrathin phase-change layers using femtosecond laser pulses. *ACS Photonics*, **1** (9), 833-839 (2014).

[4] R. Soref, Mid-infrared 2×2 electro-optical switching by silicon and germanium three-waveguide and four-waveguide directional couplers using free-carrier injection, Photonics Research 2 (5), 102-110 (2014).

[5] X. Zhao, Y. Yue, T. Liu, J. Sun, X. Wang, X. Sun, Ch. Chen, D. Zhang, Optimized design and fabrication of nanosecond response electro optic switch based on ultraviolet-curable polymers, Chin. Phys. B **24** (4) 044101 (2015).

[6] R. Won, Laser Q-switching, Nat. Photonics **8**, 422 (2014).

[7] M. Wang, J. Hiltunen, C. Liedert, S. Pearce, M. Charlton, L. Hakalahti, P. Karioja, R. Myllylä, Highly sensitive biosensor based on UV-imprinted layered polymeric-inorganic composite waveguides, Opt. Express **20** (18), 20309-20317 (2012).

[8] Y. Enami, D. Mathine, C. T. DeRose, R. A. Norwood, J. Luo, A. K.-Y. Jen, and N. Peyghambarian, Hybrid electro-optic polymer/sol-gel waveguide directional coupler switches, Appl. Phys. Lett. **94** (21), 213513 (2009).

[9] X. Wang, J. Sun, Ch. Chen, X. Sun, F. Wang D. Zhang, Thermal UV treatment on SU-8 polymer for integrated optics, Opt. Mater. Express **4** (3), 509-517 (2014).

[10] S. Lee, H.J. Shin, S.M. Yoon, D.K. Yi, J.Y. Choi, U. Paik, Refractive index engineering of transparent ZrO_2–

Unauthenticated
Download Date | 2/20/18 7:03 PM

polydimethylsiloxane nanocomposites, J. Mater. Chem. **18** (15), 1751-1755 (2008).

[11] Y. Du, L.E. Luna, W.S. Tan, M.F. Rubner, R.E. Cohen, Hollow silica nanoparticles in UV-visible antireflection coatings for poly(methyl methacrylate) substrates, ACS Nano **4** (7), 4308-4316 (2010).

[12] J.K. Plusinski, G. Lakshminarayana, Operation by acentricity in the $CdBr_2$ nanolayers, Physica E **56**, 348-350 (2014).

[13] Y.M. Alecksandrov, Y.O. Dovgii, I.V. Kityk, V.N. Kolobanov, V.N. Makhov, V.V. Mikhailin, Energy-band structure of layered $CdBr_2$ crystals, Fizika Tvardego Tela **27** (5), 1565-1567 (1985).

[14] Ya.O. Dovgii, I.V. Kityk, I.G. Man'kovskaya, L.N. Evstigneeva, Polarized light spectrum of Tl_3SbS_3 single crystals, Phys. Semicond. **24,** 1004-1005 (1990).

Received: 20 March 2015.

Unauthenticated
Download Date | 2/20/18 7:03 PM